Journal of Ceramic Processing Research. Vol. 18, No. 12, pp. 887~893 (2017)

J O U R N A L O F
Ceramic Processing Research

Effect of surfactant on wet foam stability to SiC porous ceramics

Woo Young Jang[a], Jung Gyu Park[a], In Sub Han[b], Hyung Mi Lim[c], Tae Young Lim[c] and Ik Jin Kim[a,*]

[a]*Institute of Processing and Application of Inorganic Materials, (PAIM), Department of Advanced Materials Science and Engineering, Hanseo University, 46, Hanseo 1-ro, Haemi-myun, Seosan-si, Chungchungnam-do, 31962, Korea*

[b]*Korea Institute of Energy Research (KIER), #152, Gajeong-gu, Daejeon, 34129, Korea*

[c]*Korea Institute of Ceramic Engineering & Technology(KICET), Jinju 52851, Korea*

The stabilization of wet foam is an important parameter for obtaining a large volume of dried foams in porous ceramics. Octalymine ($CH_3(CH_2)_7NH_2$) is used as a foam stabilizer, which modifies the particle surface, improves the colloidal and rheological properties of the suspension, improving the wet foam stability with a tailored bubble size. The characterization of SiC foams, including the contact angle, surface tension and adsorption free energy, Laplace pressure, foam stability, air content, bubble size, and relative bubble size are explored by changing the concentration of the ampliphile. Adsorption free energy of 1.5×10^{-15} J to nearly 1.4×10^{-14} J, and Laplace pressure of 0.52 mPa to 0.25 mPa, good wet foam stability of more than 80%, was prepared by direct foaming. Macroporous SiC ceramics with open or closed cells, an average pore size of 350 μm, 41.5% porosity and compressive strength up to 0.7 MPa were obtained when the sample was sintered at 2150 °C for 1 hr.

Key words: Colloidal suspension, Surfactant, Direct foaming, Wet-foam stability, Porous ceramics.

Introduction

The unique and excellent properties of SiC porous ceramics such as special structural properties, high strength and hardness, good mechanical properties, and excellent chemical stability, particularly at high temperatures and hostile atmospheres, makes them a superior candidate for a range of applications. These highly porous ceramics have been widely utilized in various areas such as in metallurgy as a molten metal filter, in automobile manufacturing as a diesel particulate filter, water purification filter, and diffuser, in environmental purification, in petrochemistry as a catalyst support, in fuel cells, in bioimplants, and in waste management [1-6]. The properties of cellular ceramics include a strong pore size, good pore interconnection, and good pore morphology size. Various manufacturing processes for cellular ceramics for the desired properties have been proposed, including the replica method, the sacrificial template method, and the direct foaming method [7-9].

The mechanical frothing method was used in this study for direct foaming as it is simple, versatile, has a low cost, and is ecofriendly. This method is well known and has been used in many scientific and industrial applications [10, 11] as a direct foaming technique particularly suitable for the fabrication of porous structures with a pore size between 30 mm to 1 mm^3 [12, 13]. The direct foaming method involves the production of a porous material through the direct incorporation of air into a suspension or liquid media by mechanical frothing. This generates air bubbles inside the ceramics suspension, where the bubbles are incorporated in the wet state that must be set, and usually must be sintered either in a gaseous medium or vacuum to maintain the pore structure [14, 15]. Wet-foam bubbles in colloidal suspensions are thermodynamically unstable due to the large area and high energy in the air/water interface.

Several reversible and irreversible destabilization mechanisms have been proposed, in which the bubbles tend to collapse, leaving reduced wet foam stability or no wet foam stability [15, 16]. Among them, the irreversible destabilization mechanism includes drainage, coalescence, and Ostwald ripening. Stabilization of the wet foams is achieved by in-situ hydrophobization in which apphiphilic molecules are bound to the particle surface electrostatically [17]. These molecules have a hydrophilic head group which adsorbs into the particle surface, where an ashydrophobic tail imparts the required hydrophibisity in the suspension [18].

In general, insitu hydrophobization of initially hydrophilic particles is explored to tailor the surface chemistry and stabilize the wet foam. This process enables the preparation of a wet foam with a high volume by stabilizing the particles with different chain amphiphilic molecules containing eight carbon atoms in the hydrophobic tail. The anchoring group of the molecules attaches to the particle surface and promotes the surface hydrophobization of colloidal particles [19,20].

*Corresponding author:
Tel : +82-41-660-1441
Fax: +82-41-660-1441
E-mail: ijkim@hanseo.ac.kr

The surfactant used here, octylamine ($CH_3(CH_2)_7NH_2$), adsorbs onto the SiC surface through electrostatic interaction between the positively charged surface and negatively ionized ampliphilic molecules, which provides the viscoelastic colloidal suspension with a shear thinning behavior.

In this study, the suspension stability of porous ceramics was studied as a function of zeta potential and analysis was conducted of the colloidal suspension properties, including rheological and other general colloidal properties as a function different wt.% of the surfactant added to the colloidal suspension. Particles with surfactant hydrophobized the colloidal suspension, exhibiting favorable viscous and colloidal properties. The wet foams, after being formed from the colloidal suspension, were dried at room temperature and sintered in an argon atmosphere at 2150 ºC for 1hr to tailor the microstructure of the porous ceramics. The microstructure of the cellular ceramics was characterized by using field emission scanning electron microscopy (FESEM), where the pore morphology, porosity, and pore-size distribution were analyzed.

Experimental

Materials and preparation of suspension

The initial material of SiC (d_{50} ~ 0.4 μm, density 3.21 g/cm^3, Sika Densitec, Saint Gobian, France) was mixed homogeneously in de-ionized (DI) water with a homogenizer (HM1200D, Lab stirrer, 142K, Korea) at a stirring speed of 4000 rpm for 30 min. Then, octylamine, $CH_3(CH_2)_7NH_2$ (98% Wako Pure Chemical Industries, Japan) of various wt.% (5-30 wt.%) was added to the SiC suspension as a surface modifier to hydrophobize the surfaces of the SiC particles. The slurry was mixed using a food mixer (Storming, Guang dong Xinbao Electrical, HM833, 300 W) for 1 hr at 3000 rpm. The pH of the suspension was adjusted to 10 by adding (4) M NaOH (Yakuri Pure Chemicals, Kyoto, Japan) and/or (10) N HCl (35% Yakuri Pure Chemicals, Japan) dropwise. Adding the required amount of water, the solid content of the final aqueous suspension was set to 23.8 vol.%. 20 wt.% of binder was added to the final suspension as a wet foam stabilizer. Rheological properties were examined to obtain the favorable condition for the stable colloidal suspension. After the suspension was completely mixed, the final suspension was mechanically foamed to obtain a particle stabilized wet foam, as shown in Fig. 1.

Rheological analysis

The rheological analysis of all slurries studied was carried out using a rheometer (MCR502, Anton Paar, Germany) of a cone-cup type (CC 27, cone diameter of 27 mm) and double gap type (DG26.7, cup diameter 26.7 mm) at a temperature of 25 ºC for the SiC slurry, with different concentrations of surfactant. The flow curves of the slurries were measured for shear rates from 1/sec to 1000/sec with various durations from 10 sec to 1sec for overall 120 sec. The oscillation mode and frequency sweep were measured to study the viscoelasticity. The storage modulus (G') is the elastic property of the solid, the loss modulus (G") is the viscous property of the liquid, and tan δ is defined as,

$$\tan\delta = \frac{\text{loss modulus (G'')}}{V_{Initial}\ \text{storage modulus (G')}} \quad (1)$$

where tan δ > 1 indicates liquid-like behavior

Colloidal suspension and foam characterization

The pendant-drop method (KSV Instruments Ltd., Helsinki, Finland) was used to analyze the surface tension and the contact angle of the final suspension. For the amphiphile-containing suspension, the drop volume was fixed at a constant value ranging from 5 ml to 10 ml.

The energy of the attachment, or the free energy that was gained (G) from the adsorption of a particle of the radius (r) at the interface, can be calculated using the following equation:

$$\Delta G = \pi r^2\ \gamma_{\alpha\beta}(1-\cos\theta)^2 \quad (2)$$

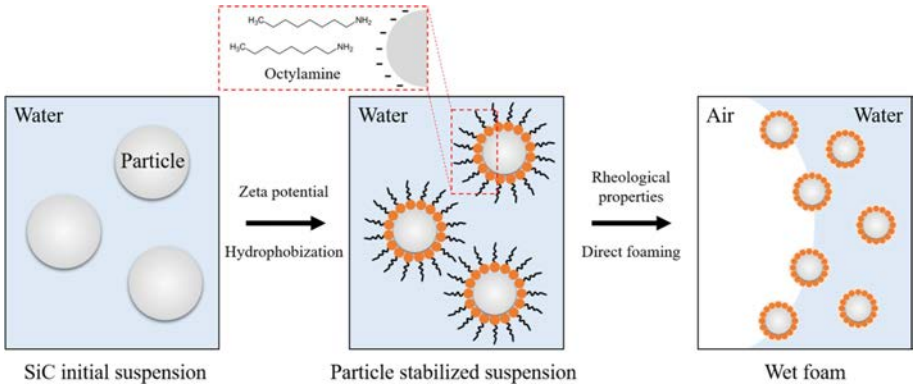

Fig. 1. Schematic diagram of direct-foaming technique to obtain SiC wet foam.

where γ is the surface tension of the suspension and θ is the contact angle. The foaming of the final suspension was carried out at room temperature, and it was achieved by using a domestic hand mixer (150 W, Super Mix, France) at highest power for 15 min. The mechanical frothing facilitated the air incorporation through the entire volume of the suspension.

The air content was calculated as a percentage of the increment of the suspension volume after the foaming, as follows:

$$Air\ content = \frac{(V_{wet\ foam} - V_{suspension}) \times 100\%}{V_{wet\ foam}} \quad (3)$$

where $V_{wet\ foam}$ indicates the wet foam volume after the foaming and $V_{suspension}$ indicates the pre-foaming suspension volume.

The results of the Laplace pressure (ΔP) imply the difference between the inner and outer pressure of the gas bubble, as follows:

$$\Delta P = \gamma\left(\frac{1}{R_1} + \frac{1}{R_2}\right) = \frac{2\gamma}{R}(Spherical\ bubble) \quad (4)$$

where γ is the surface tension of the suspension and R_1 and R_2 are the radii of the two interfacing bubbles. For the spherical-shaped bubbles, R_1 and R_2 are equal; therefore, the Laplace pressure is denoted by 2 γ/R.

To calculate the wet foam stability, the wet foam samples were poured into cylindrical molds of a consistent volume and left for 48 hrs.

The foam stability was then evaluated as a percentage upon the observation of the decrement of the foam volume, as follows:

$$Wet\ foam\ stability = \frac{V_{Final}}{V_{Initial}} \times 100\% \quad (5)$$

V_{Final} is the wet foam volume after 48 hrs, and $V_{Initial}$ indicates the wet foam volume before the 48 hrs.

The bubble size and distribution of the colloidal suspension after the 40 min mixing were evaluated using a digital camera, and the linear intercepts were measured using optical microscopy in the transmission mode (Somtech Vision, Republic of Korea). The relative bubble size was measured by calculating the percentage of the post-foaming suspension-volume increase, as follows:

$$Relative\ bubble\ size = \frac{R_{curing\ time}}{R_{Initial}} \quad (6)$$

where $R_{initial}$ is the initial-bubble radius of the colloidal suspension and $R_{curing\ time}$ is the bubble radius after the curing of the colloidal suspension for a certain period of time.

Drying, sintering, and analysis

The wet foams were dried at room temperature (22 °C to 25 °C) for 24 hr to 48 hr. After drying, the specimens were sintered at 2150 °C for 1 hr in Ar medium. The heating and cooling rates were set to 1 °C/min and 3 °C/min, respectively. The microstructures of the sintered foams were observed under a field-emission scanning electron microscope (FESEM, JEOL, Japan).

Results and Discussion

Fig. 2 shows the flow curves of the SiC slurry with different surfactant concentrations; the SiC slurry is a hydrophobic ampliphile. SiC slurry shows typical shear thinning behavior of a non-Newtonian fluid as it exhibits a decrease in viscosity with the increase in shear rate. The viscosity of the colloidal suspension increases as the surfactant concentration added to the colloidal suspension increased with an increase in shear rate. However, the suspension with higher surfactant concentration shows higher viscosity for all ranges of shear rates, and this is attributed to the considerable effect of the adsorption free energy. Adsorption free energy is always present in a colloidal system [17], and the addition of a surfactant concentration leads to a considerable increase in viscosity as the adsorption between the particles increases. The flow curve illustrates that all suspensions exhibit a typical shear-thinning behavior with a decreasing viscosity and increase in shear rate. This shear thinning behavior can be observed at low shear rates where the surface forces between particles dominate the rheological behavior [18]. As the effect of surfactant concentration, the viscosity of the suspension increases, which reflects the increases in solid content, which enhances the mechanical strength of the porous ceramics thus produced.

Fig. 3 shows the storage and loss modulus analyzed at various shear strains, with an amplitude sweep measurement in the oscillation mode. The amplitude sweep of the strain vs. modulus, the section for the linear storage modulus (G'), the Linear Viscoelastic Region(LVE) range, and the limiting value of the LVE range are selected where the storage modulus begins to decrease. The limiting shear strain of 0.02% was fixed

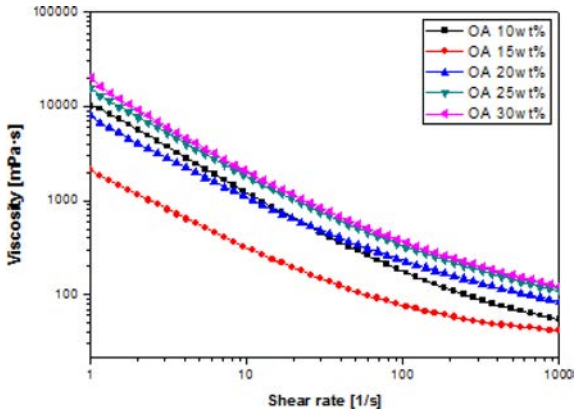

Fig. 2. Effect of the surfactant concentration on the viscosity of the colloidal suspension as a function of the shear rate.

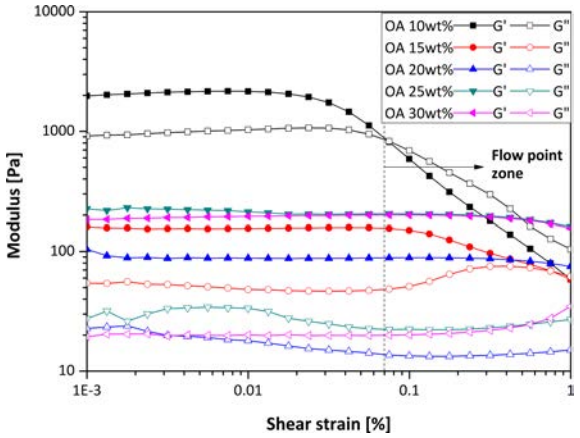

Fig. 3. Oscillation mode amplitude sweep of the slurry with surfactant concentration.

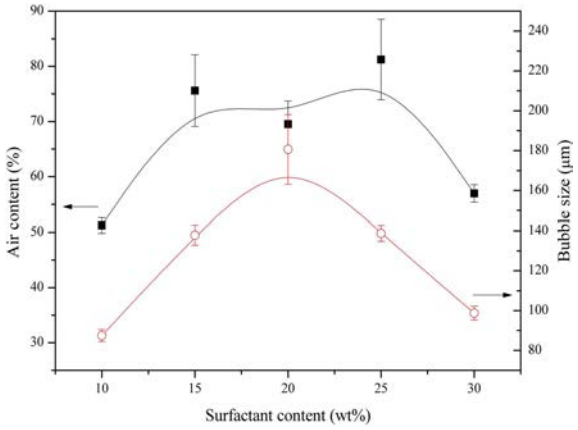

Fig. 5. Air content and bubble size with respect to the surfactant concentration in the colloidal suspension.

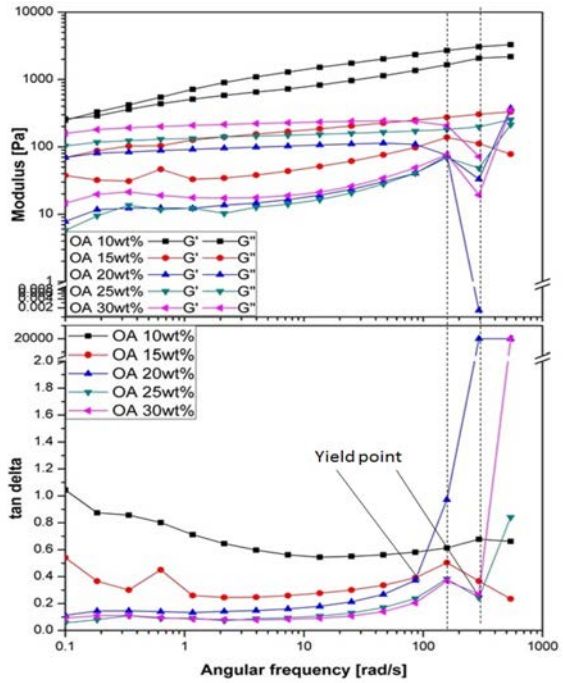

Fig. 4. Oscillation mode frequency sweep of the slurry with surfactant concentration.

to compare the frequency sweep of the slurries. The storage modulus (G') was measured to be linear and to decrease at the shear strain due to breakage of the internal structure of the material. The storage modulus (G') and the loss modulus (G") intersects each other where the flow begins, which increases as the surfactant concentration increases. The graph shows that the colloidal suspension with more than 10 wt.% of surfactant concentration forms a viscoelastic gel with a high gel strength that shows the strongest resistance to permanent deformation (yielding) under applied stress condition [19]. This composition also shows the highest wet foam stability, as shown in Fig. 8.

Fig. 4 shows the frequency sweep, measured by varying the angular frequency at a shear strain of 0.02%. Tan $\delta < 1$ indicates the solid-like behavior. The G' values of the slurries were usually higher than the G" values, and the slurries exhibited a crossover. G' and G" crossed over so that G' became lower than G", and the slurries started to flow after the crossing point. An early deviation and a vertical elevation of tan δ occur in the colloidal suspension with the higher amount of surfactant concentration in comparison to that without the surfactant or with a lower surfactant concentration, which indicates a favorable condition for the bubble formation. Fig. 4 shows G' and G" for the SiC slurry with various surfactant contents. For the slurry with surfactant, G" was only higher than G' at a high angular frequency where the slurry flowed easily. Most of the slurry behaves as a gel at a frequency of 100 rad/s or lower, and the flow behavior of these slurries was mainly dominated by the particle-particle and particle-surfactant attraction and repulsion.

Fig. 5 shows the relation between the air content and the average bubble size of the SiC suspension with respect to different surfactant concentrations. High-volume foams with an air content of up to 81% were formed with the mechanical frothing, which strongly indicates the stabilization of the wet foam due to the attachment of the particles at the air/water interface. Also, the increment in the surfactant concentration from 10 wt.% to 25 wt.% was found to be favorable with higher air content. Moreover, where the air content was slightly decreased with the decreasing bubble size and with the further increment in surfactant concentration to 30 wt.%, the air content and average bubble size decreased.

Fig. 6 shows the improvement in contact angle upon increasing the amount of surfactant. In order to produce extremely stable foams exhibiting a lifetime of several days or weeks, the colloidal particles must be adsorbed on the surface of the air bubbles. The attachment of particles at the gas-liquid interface occurs when the particles are not completely wetted; i.e. when they are partially hydrophobic. These partially hydrophobic

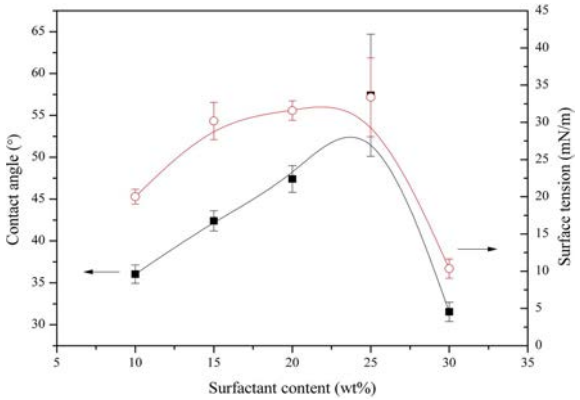

Fig. 6. Contact angle and surface tension for wet foam stability with respect to the surfactant concentration in the colloidal suspension.

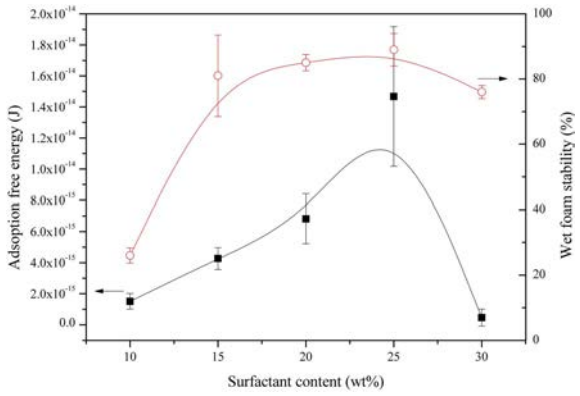

Fig. 7. Adsorption free energy for wet foam stability with respect to the surfactant concentration in the colloidal suspension.

particles are positioned primarily in the liquid phase and have a contact angle of > 90 °. From the graph in Fig. 6, it can be observed that on adding the surfactant, the contact angle of the suspension is improved from 34 ° to 58 °. However, on further addition of surfactant, it decreases drastically, which indicates the partial hydrophobization of the colloidal suspension. Correspondingly, the surface tension also increases, which indicates an increase in the surface hydrophobisity of the particle.

Fig. 7 shows the effect of the surfactant on the adsorption free energy of the colloidal suspension and the wet foam stability after the foaming. As can be seen in the figure, the energy of the attachment increased with the increase in surfactant up to 25 wt.%. A gradual increment from 2.0×10^{-15} J to 1.4×10^{-14} J can be observed compared with the colloidal suspension with 10 wt.% of surfactant, in which the energy of the attachment decreased to 1.0×10^{-15} J on further addition of surfactant up to 30 wt.%. With the increment in the concentration of the surfactant from wet foam stability increases from 26% to 82%. On increasing the surfactant concentration of 30 wt.%, the wet foam stability get reduced. From this investigation, it is confirmed that 25 wt.% of surfactant concentration was the optimum concentration for better foam stability

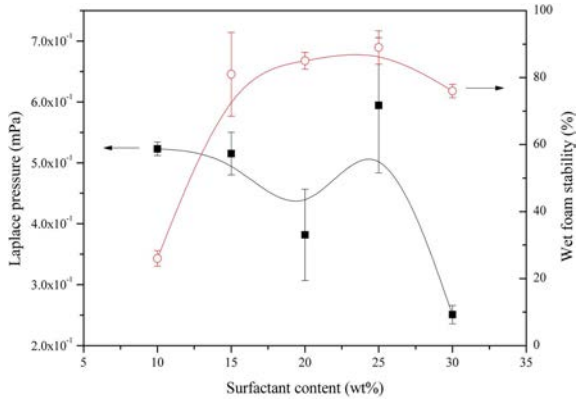

Fig. 8. Laplace pressure for the wet foam stability with respect to the surfactant concentration in the colloidal suspension.

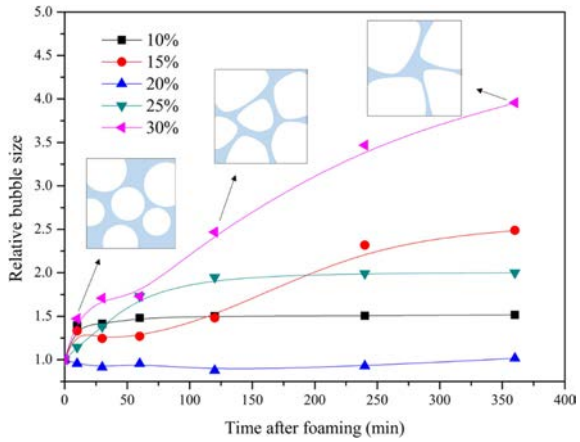

Fig. 9. Relative bubble size of SiC suspension having different surfactant concentrations with respect to the amount of time after direct foaming.

with the higher energy of attachment.

Fig. 8 shows the Laplace pressure and the wet foam stability with respect to the different surfactant concentrations. The acting pressure between two air bubbles, which results in Ostwald ripening (an important phenomenon of wet foam instability) can be measured with a Laplace-pressure evaluation [17, 18]. With the increment of the surfactant concentration, the Laplace pressure decreased, whereas the corresponding wet foam stability increased. As can be seen, the Laplace pressure decreased from 0.52 mPa to 0.38 mPa with the increase in surfactant concentration from 10 wt.% to 20 wt.%, which consistently increased to 0.59 mPa upon the addition of 25 wt.% surfactant. The further addition of surfactant decreases the Laplace pressure, which leads to the collapse of bubbles and the corresponding increase in wet foam stability from 26% to 82%. Foams with lower bubble sizes enable a higher-stability system. The highest wet foam stability of 82% was achieved when the surfactant concentration was 25 wt.%.

Fig. 9 shows the relative-bubble-size time frame of 250 min, where the bubbles tended to collapse after 1 hr due to the effect of the Ostwald ripening destabilization

mechanism that leads to the steady growth of the bubble size, thereby resulting in an unstable wet foam. The SiC colloidal suspension with surfactant concentrations of 30 wt% and 15 wt.% shows the maximum relative increase of the bubble size after 2 hrs. Also, the surfactant concentrations of 10 wt.%, 20 wt.%, and 25 wt.% are considerable with a nearly-constant relative bubble size. Also, for the corresponding adsorption between the bubbles and surfactant concentration, a minimum pressure difference between the bubbles of different sizes is necessary to ensure the stability of the foam, and to overcome defects such as coalescence and drainage [12, 14]. The experimental values also explain the pore-size increment that occurred upon the application of sintering.

The comparative micrographs of the porous ceramics with 10 wt.%, 20 wt.%, and 30 wt.% of surfactant are shown in Fig. 10. The microstructure obtained generally consists of uniformly distributed open and interconnected pores with well-developed hierarchical narrow pore size distribution. Several cell windows were covered by thin membranes, deriving from the surface modified preceramics slurry. In this comparative study, the sample with 10 wt.% surfactant showed a thick pore boundary, which reflects the poor porosity. As shown in Fig. 7, the wet foam stability was less than 30%, resulting in a thick structure, corresponding to the reduced pore distribution; even the pore size was increased up to 909.8 μm, which is the typical result of Ostwald ripening. As the surfactant concentration was increased to 20 wt.%, a narrow pore boundary was obtained with higher porosity, which was the result of higher wet foam stability. The microstructural analysis in the case of 20 wt.% surfactant also illustrates that the pore size distribution was approximately uniform, since the pore size was found to be 475 μm-575 μm. The study was further continued with the surfactant concentration of 30 wt.%. The microstructure thus obtained was found to be irregular, with a pore size distribution ranging from 265 μm to 600 μm, which results in porous ceramics with weak mechanical strength. From this comparative study, the surfactant concentration of around 20 wt.% was found to be suitable.

Since the comparative microstructural analysis showed that the preceramic slurry with the surfactant concentration of around 20 wt.% was suitable, a detailed study was carried out with surfactant concentrations of 15 wt.% and 25 wt.%. The results showed that 25 wt.% displayed better performance. The microstructural analysis of porous ceramics with 25 wt.% of surfactant at different magnifications is illustrated in Fig. 11. Interconnected pores with an average pore size of 600 μm were tailored. The mechanical properties of these SiC porous ceramics produced with 25 wt.% were found to be good. Although in the mechanical analysis, the SiC ceramics

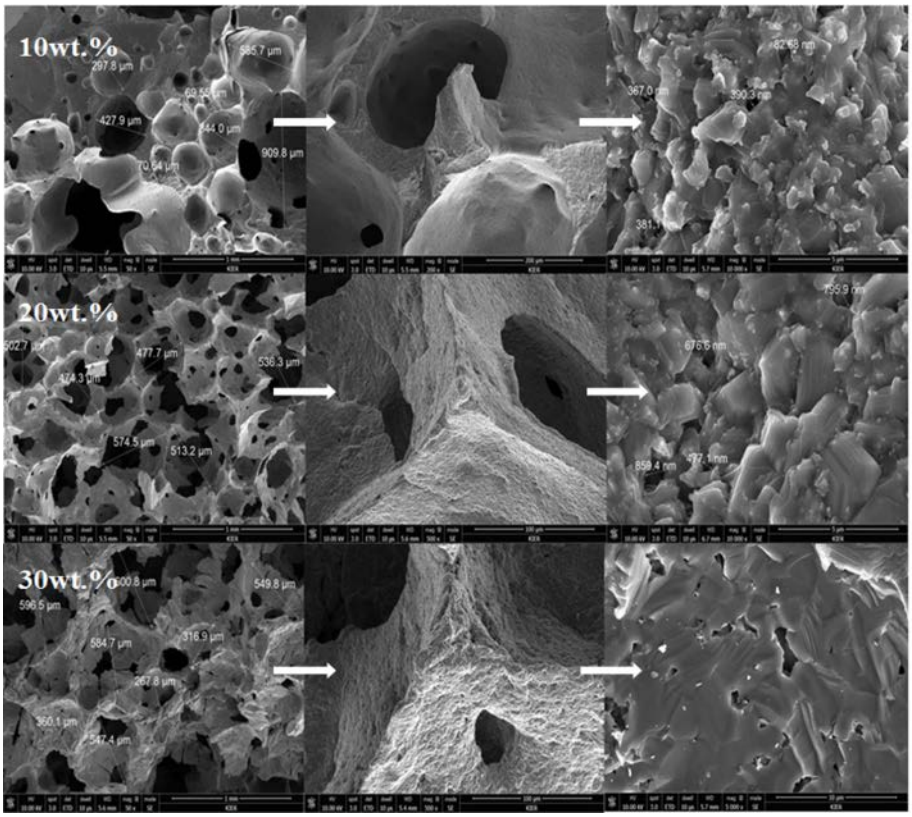

Fig. 10. FE-SEM image of SiC porous ceramics sintered at 2150 ºC for 1hr with the surfactant concentrations of 10, 20, and 30 wt% at different magnifications.

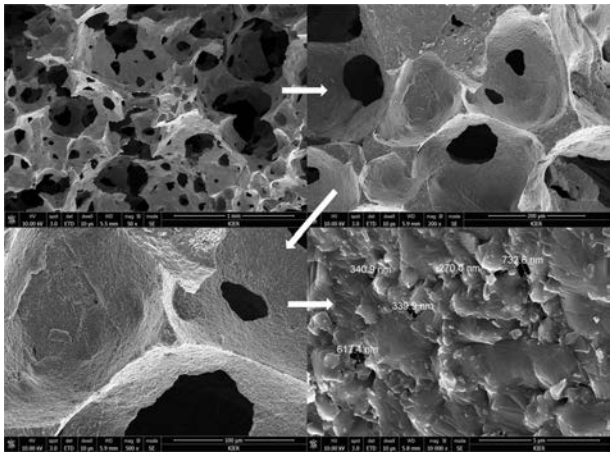

Fig. 11. FE-SEM image of porous SiC ceramics sintered at 2150 °C for 1 hr with the surfactant concentration of 25 wt% at different magnifications.

with 15 wt.% surfactant showed he comprehensive strength of 0.7 MPa and the sample with 25 wt.% surfactant only showed the comprehensive strength of 0.5 MPa, the other porous properties were superior with 25 wt.% surfactant as they showed porosity of 41.6% with a median pore diameter of 104.23 μm and bulk density of 2.172 g/ml. Highly open interconnected ceramics with fine pore boundaries were thus produced. Also, the porous ceramics sintered at higher temperature were observed to have a higher attachment, which enhanced the compatibility.

Conclusions

Porous SiC ceramics were prepared from particle stabilized wet foam using SiC powder as an initial starting material with octylamine as a surfactnat and various concentrations of surfactant. The influence of the variation of surfactant concentration (10 wt.%-30 wt.%) on the suspension stability and foam characteristics was evaluated. The addition of octylamine as an amplipliphile enabled the formation of high volume wet foam with a stability of 82%, air content of 81%, and average bubble size of 230 μm, which were achieved through direct foaming of the suspension. The increment in the surfactant shows a shear thickening behavior, which reflects the solid-like behavior of the suspension which is essential for the stability of the wet foam to achieve highly porous ceramics. The median pore diameter (at 1.74 psi and 0.096 mL/g) was found to be 104.23 μm, the bulk density found was thus 2.175 g/ml, the comprehensive strength was found to be up to 0.7 MPa, and the porosity was 41.6%.

Acknowledgments

This research was financially supported by Hanseo University and was special thanks to the research and development program of the Korea Institute of Energy Research (B6-2455) for analytical support.

References

1. X. Wu, H. Ma, X. Chen, Z. Li, and J. Li, New J. Glass Ceram. 3 (2013) 43-47.
2. M. Fukushima and P. Colombo, J. Eur. Ceram. Soc. 32[2] (2012) 503-510.
3. M. Fukushima and P. Colombo, Sci. Technol. Adv. Mater. 11 (2010) 044303.
4. K.H. Zum Gahr, R Blattner, D.H. Hwang, and K. Pohlmann, Wear 250 (2001) 299-310
5. J.H. Eom, Y.W. Kim, I.H. Song, and H.D. Kim, J. Eur. Ceram. Soc. 28 (2008) 1029-1035.
6. M. Scheffler, and P. Colombo, Cellular Ceramics, in "Structure, Manufacturing, Properties and Applications" (Weinheim, Wiley-VCH, Verlag GmbH & Co. KGaA, 2005) p.645.
7. A.R. Studart, U T. Gonzenbach, E. Tervoort, and L. J. Gauckler, J. Am. Ceram. Soc. 89[6] (2006) 1771-1789.
8. J.C.H. Wong, E. Tervoort, S. Busato, U.T. Gonzenbach, A.R. Studart, P. Ermanni, and L.J. Gauckler, J. Mater. Chem. 20 (2010) 5628-5640.
9. R. Mouazer, S. Mullens, I. Thijs, J. Luyten, and A. Buekenhoudt, Adv. Eng. Mater. 7[12] (2005) 1124-1128.
10. M. Vecer, and J. Pospisil, Procedia Eng. 42 (2012) 1720-1725.
11. Z. Yuan, Y Zhang, Y. Zhou, and S. Dong, RSC Adv. 4 (2014) 50386.
12. J.S. Lee, S.H. Lee, and S.C. Choi, J. Alloys Compd. 467 (2009) 543-549.
13. K. Ohenoja, J. Saari, M. Illikainen, S. B. Faes, A. Kwade, and J. Niinimäki, Chem. Eng. Technol. 37[5] (2014) 833-839.
14. F. Li, Z. Kanga, X. Huanga, X.G. Wang, and G.J. Zhang, J. Eur. Ceram. Soc. 34 (2014) 3513-3520.
15. N. Sarkar, J.G. Park, S. Mazumder, D.N. Seo, and I. J. Kim, Ceram. Int. 41 (2015) 4021-4027.
16. L.Y. Zhang, D.l. Zhou, Y. Chen, B. Liang, and J. B. Zhou, J. Eur. Ceram. Soc. 34 (2014) 2443-2452.
17. A. Pokhrel, S.D. Nam, S.T. Lee and I.J. Kim, J. Korean Ceram. Soc. 50[2] (2013) 93-102.
18. B.S. Murray, Curr. Opin. Colloid Interface Science. 12 (2007) 231-241.
19. T.S. Horozov, Curr. Opin. Colloid Interface Science 13 (2008) 134-40.
20. R.L. Menchavez, C.R.M. Adavan, and J. M. Calgas, Mater. Res. 17[1] (2014) 157-167.
21. A.R. Patel, B. Mankoc, M.D. Bin Sintang, A. Lesafferb and K. Dewettincka, RSC Adv. 5 (2015) 9703.
22. I. Butnaru, M.P. Fernández-Ronco, J.C. Polak, M. Heneczkowski, M. Bruma, and S. Gaan, Polym. 7 (2015) 1541-1563.